Pergamon

Int. J. Heat Mass Transfer. Vol. 40, No. 1, pp. 89–99, 1997
Copyright © 1996 Elsevier Science Ltd
Printed in Great Britain. All rights reserved
0017-9310/97 $15.00+0.00

PII: S0017-9310(96)00074-9

Ignition phenomenon of solid fuel in a confined rectangular enclosure

SEUNG WOOK BAEK and TAIK YOUNG KIM

Korea Advanced Institute of Science and Technology, Aerospace Engineering Department, 373-1 Gusung-dong, Yusung-ku, Taejon, Korea

and

CAROLYN R. KAPLAN

Navy Technology Center for Safety/Survivability, Naval Research Laboratory, Washington, DC 20375, U.S.A

(*Received* 14 *June* 1995 *and in final form* 8 *February* 1996)

Abstract—In this study the ignition model of a PMMA (polymethyl-methacrylate) wall has been proposed in a two-dimensional rectangular enclosure when it is initially exposed to a high-temperature source. The effect of surface radiation has been taken into account. It was found that the transient development of thermo-fluid fields was strongly governed by wall heating due to surface radiation. In particular, the rapid heating of the adiabatic floor made the flow very unstable, creating complex secondary recirculating flows. Depending on the hot source temperature, the ignition process was controlled either by mixing and transport of fuel vapor and oxidizer in the vicinity of the hot wall, or by infiltration of hot air into the region near the PMMA wall. Copyright © 1996 Elsevier Science Ltd.

1. INTRODUCTION

Ignition of organic solids exposed to a high temperature heat source is one of many interesting topics in the fire safety area. Due to the severe financial and environmental damage incurred by a fire hazard, it would be very beneficial to determine how to diminish the potential danger of ignition.

When an organic solid is heated, it starts to be pyrolysed while ejecting volatile gases. The volatile gases are then diffused and/or convected to mix with the oxidizer in the surrounding air. As this mixture is chemically or thermally provoked, the onset of ignition takes place. Therefore, the ignition process of pyrolysing organic solid fuel is considered to be a very complex phenomenon comprised of heat and mass transfer as well as chemical reaction.

During the past decades many studies have reported on the ignitability of various materials and their ignition mechanisms. Simms [1] empirically explored the radiative ignition of cellulosic materials such as wood and paper. It was shown that ignition was first observed in the gas phase and that the external convective drafts and exhaustion of volatile gases are important factors to determine whether or not ignition can occur. Martin [2] carried out an experimental study with cellulosic materials and showed the importance of gas phase ignition. The effect of free convection on the ignition of a vertical cellulosic panel by thermal radiation has been studied by Alvares *et al.* [3].

A great deal of work was performed with PMMA (polymethyl-methacrylate) or other plastic materials in diverse fire related research studies. Kashiwagi [4] investigated radiation-induced ignition by considering the detailed radiation effects of the solid fuel and discussed the ignitable domain as a function of several different parameters. An experimental study of radiative ignition was also carried out for two types of orientation [5]. The ignition delay times were found to be shorter for a horizontal sample than for a vertical one at the same external radiant flux. Gas phase ignition in a boundary layer along a vertical plate was examined by Gandhi and Kanury [6] while considering the effect of natural convection. A one-dimensional transient ignition model including gas phase radiation as well as in-depth radiation of a solid fuel was also proposed by Park and Tien [7]. Because gas phase radiation was included, a different type of ignitable domain was obtained in comparison with the work by Kashiwagi [4]. Baek and Kim [8] discussed the gas phase ignition of pyrolysing PMMA exposed to a radiative source in a one-dimensional slab geometry. The emissivity of the hot radiation source was observed to play a significant role in the ignition process.

Whereas all of the aforementioned studies were performed in open environments, many practical problems related to fire research are taking place in confined geometries. In principle, the ignition problem has a very close link with the natural convection problem. Unsteady natural convection in a rectangular enclosure is a long-standing topic in the area of fluid

NOMENCLATURE

A	pre-exponential factor for gaseous reaction
c_p	specific heat at constant pressure
D	species diffusion coeffieicnt
E_a	activation energy for gaseous reaction
E_P	activation energy for pyrolysis
F	configuration factor
g	gravity
G	irradiation
h	sensible enthalpy
H	height
J	radiosity
L_h	latent heat of pyrolysis
Nu	Nusselt number
p	pressure
q	heat flux
Ra	Rayleigh number
R	gas constant
R_u	universal gas constant
t	time
T	temperature
u, v	velocity
W	molecular weight
x, y	coordinates
Y	mass fraction
Z	pre-exponential factor for pyrolysis.

Greek symbols

α_P	thermal diffusivity of PMMA
β	volumetric coefficient of thermal expansion
ε	emissivity
λ	thermal conductivity
μ	dynamic viscosity
ρ	density
Φ	viscous dissipation function
σ_{ji}	stress tensor
ω	reaction rate.

Superscripts

C	conduction
P	pyrolysis
R	radiation
T	net.

Subscripts

F	fuel
h	hot wall
O	oxidizer
s	interface of PMMA
w	wall.

mechanics and heat transfer. An oscillatory mode of solution converging to a final steady state condition was found to exist for certain flow regimes by Ivey [9]. It was argued that this oscillatory behavior is due to the inertia of the flow entering the interior of the cavity from the side wall boundary layers, which may lead to a form of hydraulic jump if the Rayleigh number ($Ra = g\beta\Delta TH^3/\nu\alpha$) is sufficiently large.

When surface radiation takes part in heat exchange among the walls, the basic nature of the flow becomes totally different from the case in which no radiation is involved. The rapid heating of the walls due to absorption of radiation would make the flow locally unstable, so that a very complicated fluid motion would be incurred during the initial period. This would enhance the development of thermo-fluid fields. By the same reasoning, the radiation would reduce the heating time required for a solid fuel to be pyrolysed in an ignition process within a confined geometry.

In order to elucidate these concepts in this work, the radiative and convective ignition of a vertical wall composed of solid fuel is numerically analysed in a confined rectangular enclosure. Convective and radiative wall heating, evolution of volatile gases from the solid fuel, their mixing with ambient air by diffusion and convection, and the eventual ignition process (where an appropriate thermal condition is met) are all addressed. To the authors' best knowledge, this work represents the first approach in modeling transient radiative and natural convection ignition in a confined geometry.

2. ANALYSIS

In order to investigate the ignition phenomenon by convection and radiation in a rectangular enclosure, consider a schematic diagram of the physical domain, depicted in Fig. 1. Initially the enclosed air and all of the wall boundaries are assumed to be held at ambient temperature and the air is stagnant. At time $t > 0$, the temperature of the left-hand side wall is increased to T_h. Both the upper wall (ceiling) and the lower wall (floor) are considered adiabatic and the right-hand side wall is a combustible solid composed of PMMA. The involved gas would begin to be naturally convected near the very high temperature wall. But instead of adopting the Boussinesq approximation, as is commonly done in solving natural convection problems, the ideal gas equation is utilized. The transport properties of air are allowed to vary depending on temperature, as given in Table 1. As the PMMA wall is heated by convection and surface radiation from the other walls, the ejected fuel vapor is continuously supplied to the surrounding air, thereby increasing the pressure. Therefore, the pressure and

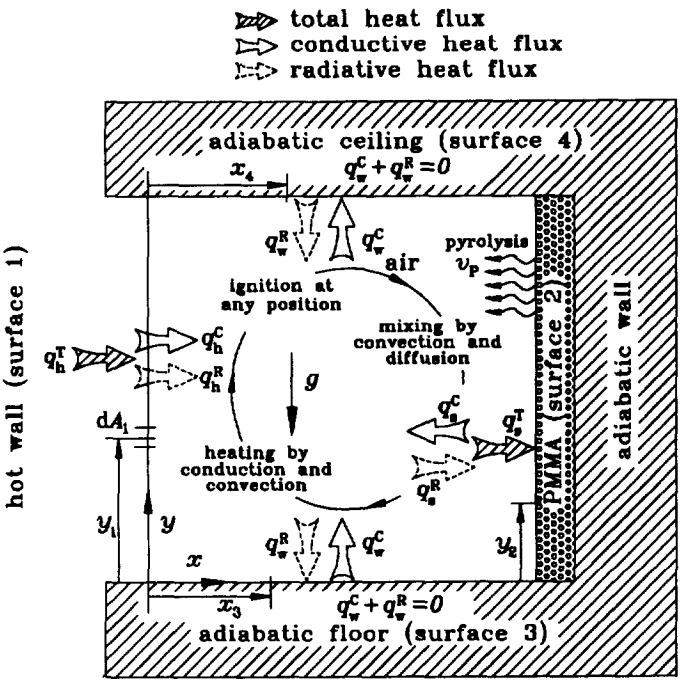

Fig. 1. Schematic diagram of the physical and geometrical domain.

Table 1. Transport properties of air

Property of gas (air)	Symbol	Value
Density	ρ(at 300 K)	1.177 [kg m^{-3}]
Heat of formation for fuel	$\Delta h^{\circ}_{f,F}$	2.6×10^{7} [J kg^{-1}]
Pre-exponential factor for gaseous reaction	A	1.6×10^{15} [kg K^{2} m^{-3} s^{-1}]
Activation energy for gaseous reaction	E_2	1.8×10^{8} [J kg^{-1} mole^{-1}]
Universal gas constant	R_u	8314.4 [J kg^{-1} mole^{-1} K^{-1}]
Lewis number	$Le=\lambda/\rho c_P D$	1 (constant)
Dynamic viscosity	$\mu=\dfrac{14.58\times10^{-7}T^{3/2}}{110.4+T}$	[kg m^{-1} s^{-1}]
Thermal conductivity	$\lambda=\dfrac{2.6482\times10^{-3}T^{1/2}}{1+245.4\times10^{-12/T}/T}$	[W m^{-1} K^{-1}]
Specific heat	$c_P=917-0.258T-0.398\times10^{-4}T^{2}$	[J kg^{-1} K^{-1}]

dissipation terms are not neglected in the energy equation below.

According to the assumptions mentioned above, the governing equations for the gas can be expressed as follows:

continuity equation

$$\frac{\partial\rho}{\partial t}+\frac{\partial\rho u_i}{\partial x_i}=0 \tag{1}$$

momentum equation

$$\frac{\partial\rho u_j}{\partial t}+\frac{\partial\rho u_i u_j}{\partial x_i}=-\frac{\partial p}{\partial x_j}+\frac{\partial\mu\sigma_{ji}}{\partial x_i}+\rho f_j \tag{2}$$

energy equation

$$\frac{\partial\rho h}{\partial t}+\frac{\partial\rho u_i h}{\partial x_i}=\frac{\partial}{\partial x_i}\left(\lambda\frac{\partial T}{\partial x_i}\right)+\frac{\partial p}{\partial t}+u_i\frac{\partial p}{\partial x_i}+\mu\Phi+\frac{\partial}{\partial x_i}\left(\rho D\sum_k\frac{\partial Y_k}{\partial x_i}h_k\right)-\sum_k\Delta h^{o}_{f,k}\omega_k \tag{3}$$

species conservation equation

$$\frac{\partial\rho Y_k}{\partial t}+\frac{\partial\rho u_i Y_k}{\partial x_i}=\frac{\partial}{\partial x_i}\left(\rho D\frac{\partial Y_k}{\partial x_i}\right)+\omega_k \tag{4}$$

equation of state

$$p = R\rho T \tag{5}$$

where the gravity force, f_j, stress tensor, σ_{ji}, and dissipation finction, Φ are written as:

$$f_j = \begin{Bmatrix} f_x = -g\sin\varphi \\ f_y = -g\cos\varphi \end{Bmatrix}$$

$$\sigma_{ji} = \left(\frac{\partial u_j}{\partial x_i} + \frac{\partial u_i}{\partial x_j}\right) - \frac{2}{3}\frac{\partial u_l}{\partial x_l}\delta_{ji}$$

$$\Phi = \sigma_{ji}\frac{\partial u_i}{\partial x_j} = 2\delta_{ji}\left(\frac{\partial u_i}{\partial x_j}\right)^2 + \left[(1-\delta_{ji})\frac{\partial u_i}{\partial x_j}\right]^2 - \frac{2}{3}\left(\frac{\partial u_i}{\partial x_i}\right)^2. \tag{6}$$

The multi-component diffusion coefficient, D, was assumed to be equal for fuel and oxidizer. φ is the inclination angle between gravity direction and coordinate. The exothermic gas phase reaction of the fuel is modeled by a single step of the form

$$v_F M_F + v_O M_O \rightarrow v_P M_P \tag{7}$$

with a global second-order reaction rate described by Arrhenius kinetics:

$$\omega_F = \frac{v_F W_F}{v_O W_O}\omega_O = -A Y_F Y_O T^{-2}\exp\left(-\frac{E_a}{R_u T}\right). \tag{8}$$

In order to illustrate the thermal decomposition of the right-hand side PMMA wall, the following two-dimensional transient form of the energy equation for the solid fuel is solved

$$\frac{\partial T_P}{\partial t} = \alpha_P\left(\frac{\partial^2 T_P}{\partial x^2} + \frac{\partial^2 T_P}{\partial y^2}\right). \tag{9}$$

Corresponding initial conditions for the gas and solid fuel are

$$\begin{aligned} &u = v = 0\ \mathrm{m\,s^{-1}}, \\ &h = 0\ \mathrm{J\,kg^{-1}} \quad (\text{from } T = 300\ \mathrm{K}) \\ &\rho = 1.177\ \mathrm{kg\,m^{-3}} \quad Y_F = 0 \\ &Y_O = 0.232 \quad T_P = 300\ \mathrm{K}. \end{aligned} \tag{10}$$

The boundary conditions for the gas phase governing equations are given as follows:

at $x = 0$ m (wall with heat source)

$$u = v = 0\ \mathrm{m\,s^{-1}}$$

$$h = h_h\ \mathrm{J\,kg^{-1}} \quad (\text{from } T = T_h\ \mathrm{K})$$

$$\frac{\partial Y_F}{\partial x}\Big|_w = \frac{\partial Y_O}{\partial x}\Big|_w = 0$$

at $x = L$ m (PMMA wall)

$$u = -v_P\ \mathrm{m\,s^{-1}} \quad v = 0\ \mathrm{m\,s^{-1}}$$

$$h = h_s\ \mathrm{J\,kg^{-1}}$$

$$\left(\text{from } -\lambda\frac{\partial T}{\partial x}\Big|_s - q_s^R - \rho v_P L_h - \lambda_P\frac{\partial T_P}{\partial x}\Big|_s = 0\right)$$

$$-\rho v_P = -\rho v_P Y_{F,s} - \rho D\frac{\partial Y_F}{\partial x}\Big|_s$$

$$0 = -\rho v_P Y_{O,s} - \rho D\frac{\partial Y_O}{\partial x}\Big|_s$$

at $y = 0$ m and $y = H$ m (adiabatic walls)

$$u = v = 0\ \mathrm{m\,s^{-1}}$$

$h = h_w\ \mathrm{J\,kg^{-1}}$ (from $q_w^T = q_w^C + q_w^R = 0$; adiabatic condition)

$$\frac{\partial Y_F}{\partial y}\Big|_w = \frac{\partial Y_O}{\partial y}\Big|_w = 0. \tag{11}$$

The boundary conditions for the solid fuel energy equation are

$$\begin{aligned} &T = T_{P,s}\ \mathrm{K} \quad (\text{at } x = 0\ \mathrm{m}) \\ &\frac{\partial T_P}{\partial x}\Big|_w = 0 \quad (\text{at } x = \delta\ \mathrm{m}) \\ &\frac{\partial T_P}{\partial y}\Big|_w = 0 \quad (\text{at } y = 0, H\ \mathrm{m}) \end{aligned} \tag{12}$$

where δ is the thickness of the solid fuel.

As the PMMA wall is heated, it is thermally decomposed. The volatile gases formed are then mixed with the enclosed air. The rate of pyrolysis is assumed to be governed by a first-order Arrhenius type expression as follows:

$$\rho v_P = Z\exp\left(-\frac{E_P}{R_u T_{P,s}}\right). \tag{13}$$

The thermo-physical properties of PMMA are listed in Table 2 [10, 11]. In order to keep the flow laminar, the height and length of the rectangular enclosure are assigned values of 0.1 m, respectively. The thickness of PMMA is considered to be 0.01 m.

In this work, since the direct exchange of radiative energy is assumed among the gray walls involved, it is necessary to account for the radiative heat flux at each wall. The radiative heat flux q^R at the jth gray wall with an arbitrary temperature distribution can be written as

$$q_j^R(s) = J_j(s) - G_j(s) \tag{14}$$

where G and J represent the irradiation and radiosity, respectively. There is the following relation between irradiation and radiosity:

$$J_j(s) = \varepsilon_j\sigma T_j^4(s) + (1-\varepsilon_j)G_j(s) \tag{15}$$

$$\mathrm{d}A_j G_j(s) = \sum_{i=1}^{4}\int_{A_i} J_i(s)\,\mathrm{d}A_i\,\mathrm{d}F_{i-j} \tag{16}$$

Table 2. Thermo-physical properties of polymethylmethacrylate (PMMA)

Property of PMMA	Symbol	Value
Density	ρ_P	1.17×10^{3} [kg m^{-3}]
Specific heat	c	1.22×10^{3} [J kg^{-1} K^{-1}]
Thermal diffusivity	$\alpha_P=\lambda_P/\rho_P c$	1.296×10^{-6} [m^2 s^{-1}]
Latent heat of pyrolysis	L_h	1.007×10^{6} [J kg^{-1}]
Pre-exponential factor for pyrolysis	Z	3.6×10^{12} [kg m^{-2} s^{-1}]
Activation energy for pyrolysis	$E_{a,P}$	1.8×10^{8} [J kg^{-1} mol^{-1}]
Surface emissivity	$\varepsilon_{w,P}$	0.92
Stefan–Boltzmann constant	σ	5.6699×10^{-8} [W m^{-2} K^{-4}]

where ε_j, dA_j and dF_{i-j} are the wall emissivity, the differential area of the jth wall and the geometric configuration factor defined as a fraction of energy leaving the elemental surface area dA_i that arrives at the surface element dA_j, respectively. Whereas a black body is assumed for the hot left-hand side wall with an emissivity of unity, the emissivities of the adiabatic ceiling and floor are both set to 0.8. The PMMA wall emissivity is 0.92. There is a reciprocity relation governing the geometric configuration factors

$$dA_i\,dF_{i-j}=dA_j\,dF_{j-i}. \tag{17}$$

From equations (14)–(17), the following relations can be obtained

$$J_j(s)=\varepsilon_j\sigma T_j^4(s)+(1-\varepsilon_j)\sum_{i=1}^{4}\int_{A_i}J_i(s)\,dF_{j-i} \tag{18}$$

$$q_j^R(s)=\frac{\varepsilon_j}{1-\varepsilon_j}\left[\sigma T_j^4(s)-J_j(s)\right]. \tag{19}$$

According to the geometric coordinates in Fig. 1, the geometric configuration factors can be deduced as the following:

$$\frac{dF_{1-2}}{dA_2}=\frac{dF_{2-1}}{dA_1}=\frac{1}{2}\frac{L^2}{[L^2+(y_2-y_1)^2]^{3/2}}$$

$$\frac{dF_{1-3}}{dA_3}=\frac{dF_{3-1}}{dA_1}=\frac{1}{2}\frac{y_1x_3}{\left(x_3^2+y_1^2\right)^{3/2}}$$

$$\frac{dF_{1-4}}{dA_4}=\frac{dF_{4-1}}{dA_1}=\frac{1}{2}\frac{(H-y_1)x_4}{\left[x_4^2+(H-y_1)^2\right]^{3/2}}$$

$$\frac{dF_{2-3}}{dA_3}=\frac{dF_{3-2}}{dA_2}=\frac{1}{2}\frac{y_2(L-x_3)}{\left[(L-x_3)^2+y_2^2\right]^{3/2}}$$

$$\frac{dF_{2-4}}{dA_4}=\frac{dF_{4-2}}{dA_2}=\frac{1}{2}\frac{(H-y_2)(L-x_4)}{[(H-y_2)^2+(L-x_4)^2]^{3/2}}$$

$$\frac{dF_{3-4}}{dA_4}=\frac{dF_{4-3}}{dA_3}=\frac{1}{2}\frac{H^2}{[H^2+(x_4-x_3)^2]^{3/2}}$$

$$dF_{i-i}=0. \tag{20}$$

The gas phase governing equations are numerically solved by the well-known SIMPLER algorithm [12] using the QUICK scheme [13] for the convective term. The algebraic equations for the radiative heat flux are solved by direct inversion of the full matrix. A 61×61 nonuniform grid is adopted for the gas phase calculation, with computational cells clustered near the wall region, whereas a 15×61 uniform grid is used for the solid fuel region.

3. RESULTS AND DISCUSSION

The onset of ignition of the thermally decomposed volatile gases would be strongly affected by the evolution of the thermo-fluid field due to the hot wall source. In the following discussion, therefore, the ignition mechanism is investigated for various temperatures of the heat source.

Figure 2 illustrates the temporal development of velocity vectors, isotherms, mass fraction and reaction rate (with stoichiometric line) for a hot wall temperature of 1000 K. It must be noted that surface radiation is taken into account in this study. Initially a very steep temperature gradient is formed along the hot wall surface. Simultaneously the thermal boundary layer is also developing at the adiabatic ceiling and floor, since the surface radiation instantly heats the other inner surfaces. The velocity boundary layer is also evolving near the hot wall due to the buoyancy effects. The location where the maximum velocity occurs is represented by the circle in the figure. The uprising flow in this layer drives the stratified temperature field in the upper zone of the enclosure. This upward flow then turns in a downward direction due to blockage by the ceiling wall. The right-hand side PMMA wall surface is also exposed to incident radiation from the other walls. While one part is transmitted into the solid fuel by conduction, the remaining part is delivered to the air. The PMMA fuel is thus continuously heated to reach its pyrolysing temperature. The heat supplied to the air induces another free convective boundary layer at $t=0.6$ s. As the bottom wall continues to be heated, a rising current of air develops. This rising motion from the floor provokes a very complex recirculating flow pattern, starting from $t=0.6$ s. As the upward gas flow is getting

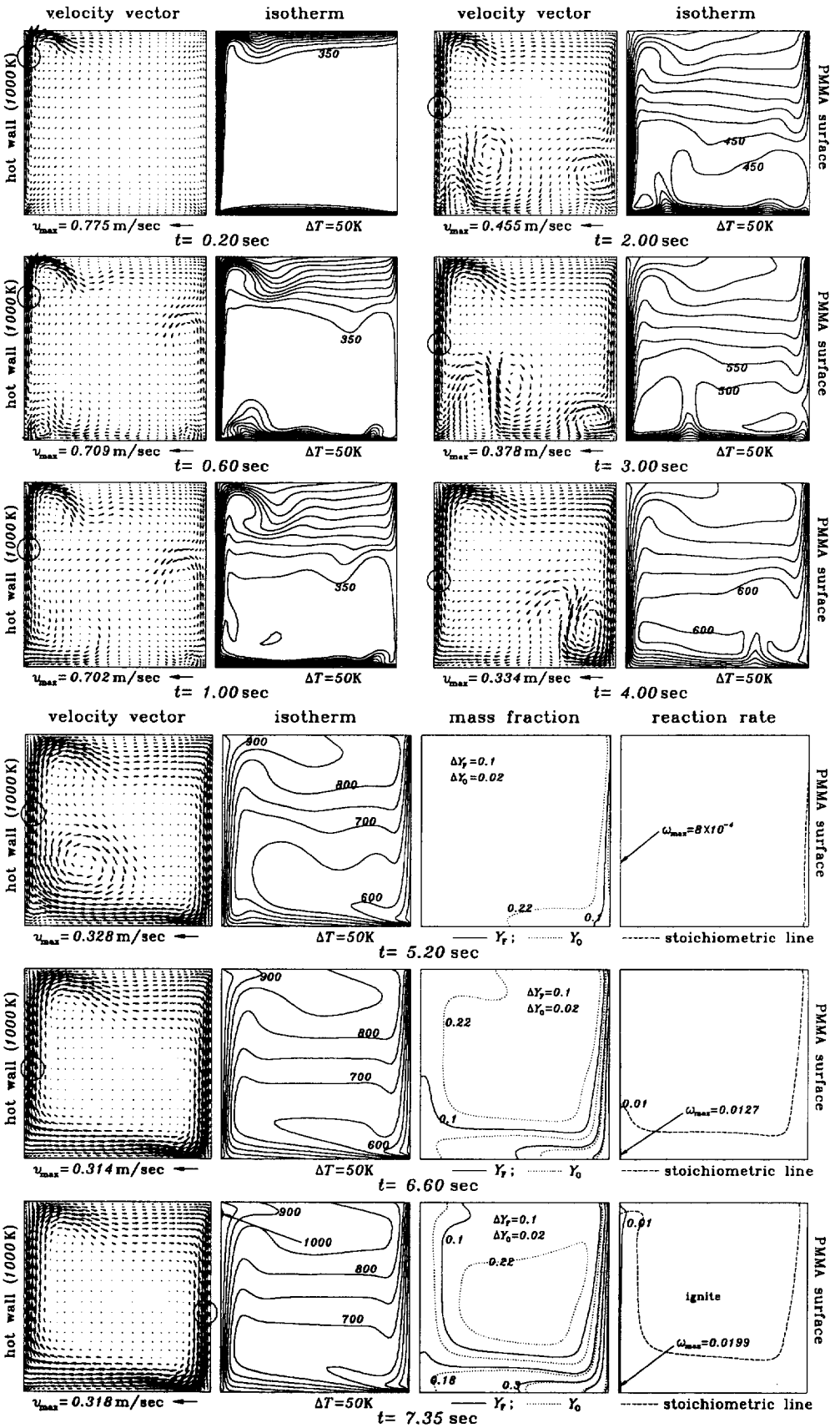

Fig. 2. Temporal variations of velocity vector, isotherm, fuel and oxidizer mass fractions and reaction rate with stoichiometric line for hot wall temperature, T_h = 1000 K.

stronger near the hot wall, it provides momentum, which induces the downward gas motion along the right-hand side PMMA wall, as shown in the figure at $t = 4.0$ s.

At $t = 5.2$ s, the PMMA wall is being pyrolysed along the surface. The pyrolysed fuel vapor is convected towards the hot wall, along with the main convective currents, while being mixed with air. A significant amount of reaction is observed at the upper-left corner in the reaction rate plot at 7.35 s. Although the stoichiometric line is already in contact with the lower part of the hot wall before $t = 6.6$ s, as shown in the reaction rate plot, an appreciable amount of reaction (ignition) is taking place when the stoichiometric line reaches the upper part of the hot wall. At $t = 5.2$ s, the plots shows that ignition cannot be incurred even though there exists a stoichiometric mixture, since the local temperature is lower than 800 K near the PMMA wall. This is consistent with the results shown by Kim [14], that no exothermic reaction takes place throughout the developing period when the hot wall temperature is lower than 900 K. Once the stoichiometric mixture reaches the area near the hot wall, it is promptly displaced in the upward direction due to a relatively high local velocity, as seen in the figures for $t = 6.6$ and 7.35 s. As the stoichiometric line is convected along the hot wall, more stoichiometric mixture is established and simultaneously heated in the vicinity of the hot wall. In the region below the stoichiometric line, a fuel rich mixture exists. Ignition is therefore taking place only after enough of the stoichiometric mixture is produced by mixing. The ignition process is thus considered to be primarily controlled by mixing and transport of fuel and oxidizer.

When the hot wall temperature is increased to 1100 K, a more complicated variation of thermo-fluid variables is observed, as shown in Fig. 3. The rising fluid motion from the bottom wall and the resulting secondary recirculation flows are seen to be more vivid and stronger, which would enhance the mixing of fuel and oxidizer. The rate of evolution of fuel vapor is also faster. Thus the stoichiometric mixture is more widely distributed in the enclosure. A considerable amount of reaction is beginning to occur at $t = 4.0$ s, as there exists a small amount of fuel vapor at the hot wall. However, at this time, the stoichiometric line is not yet in contact with the hot wall. As time passes, more fuel vapor is convected into the hot wall region and the reaction proceeds all along the hot wall. When the stoichiometric line comes in contact with the hot wall, the flame would develop and exist along the stoichiometric mixture.

When the hot wall temperature is further increased past 1100 K, a different type of ignition mechanism is observed. This is shown in Fig. 4, for the case in which the hot wall temperature is 1300 K. Due to the effect of strong surface radiation, the thermal boundary layer is seen to be developing at all of the walls. A strong upward fluid motion is induced at the PMMA wall, which starts to be pyrolysed at an early time. The evolved fuel vapor is mixed with oxidizer by convection and diffusion. However, in this case, the uprising fluid motion from the bottom wall does not contribute to the mixing phenomenon mentioned above.

While the stoichiometric line is diffusing out vertically from the PMMA wall following the fluid motion, the reaction starts near the right-upper corner. Here the movement of fuel vapor is quite different from the previous two cases. It results from the strong natural convection along the PMMA wall caused by the strong effect of surface radiation. Consequently the generated fuel vapor does not move in the clockwise direction to the hot wall region. Rather, the high temperature thermal region originating from the hot wall steadily grows to reach the PMMA wall, where a reasonable amount of fuel and oxidizer exists. Eventually, the onset of ignition is prompted at this PMMA wall. Thus, this ignition process is considered to be thermally controlled, which is different from the two previous cases.

To investigate the characteristics of heat transfer and PMMA pyrolysis, the Nusselt number, mean temperature and mean ejecting velocity along the PMMA surface are defined such as

$$Nu_s^T = Nu_s^C + Nu_s^R + Nu_s^P = \frac{1}{H}\int_0^H \left\{\frac{q_w^C}{\lambda(T_h - T_o)}\right\}_{x=L} dy + \frac{1}{H}\int_0^H \left\{\frac{q_w^R}{\lambda(T_h - T_o)}\right\}_{x=L} dy + \frac{1}{H}\int_0^H \left\{\frac{-\rho v_P L_h}{\lambda(T_h - T_o)}\right\}_{x=L} dy \quad (21)$$

$$v_{P,m} = \frac{1}{H}\int_0^H v_P\, dy, \quad T_{P,m} = \frac{1}{H}\int_0^H T_P\, dy \quad (22)$$

where superscripts T, C, R and P denote the net, conductive, radiative and pyrolysis terms. The first and second terms on the right-hand side of equation (21) represent the conductive and radiative heat fluxes toward the PMMA surface. The last term (with the negative sign) represents the heat required for PMMA to be thermally decomposed.

Figure 5 shows a temporal variation of these variables versus time on a logarithmic scale for various hot wall temperatures ranging from 900 K to 1350 K. Initially the positive radiative term is slightly larger than the net term, as shown in the figure. This means that the PMMA wall is predominantly heated by radiation from the other walls. The temperature of the PMMA wall therefore becomes higher than that of the surrounding gas. Subsequently this results in net conductive heat transfer from the PMMA wall to gas, which is represented by the negative value of Nu^C. In the initial heating period, the fraction of incident radiant flux, which is provided back to the air is small,

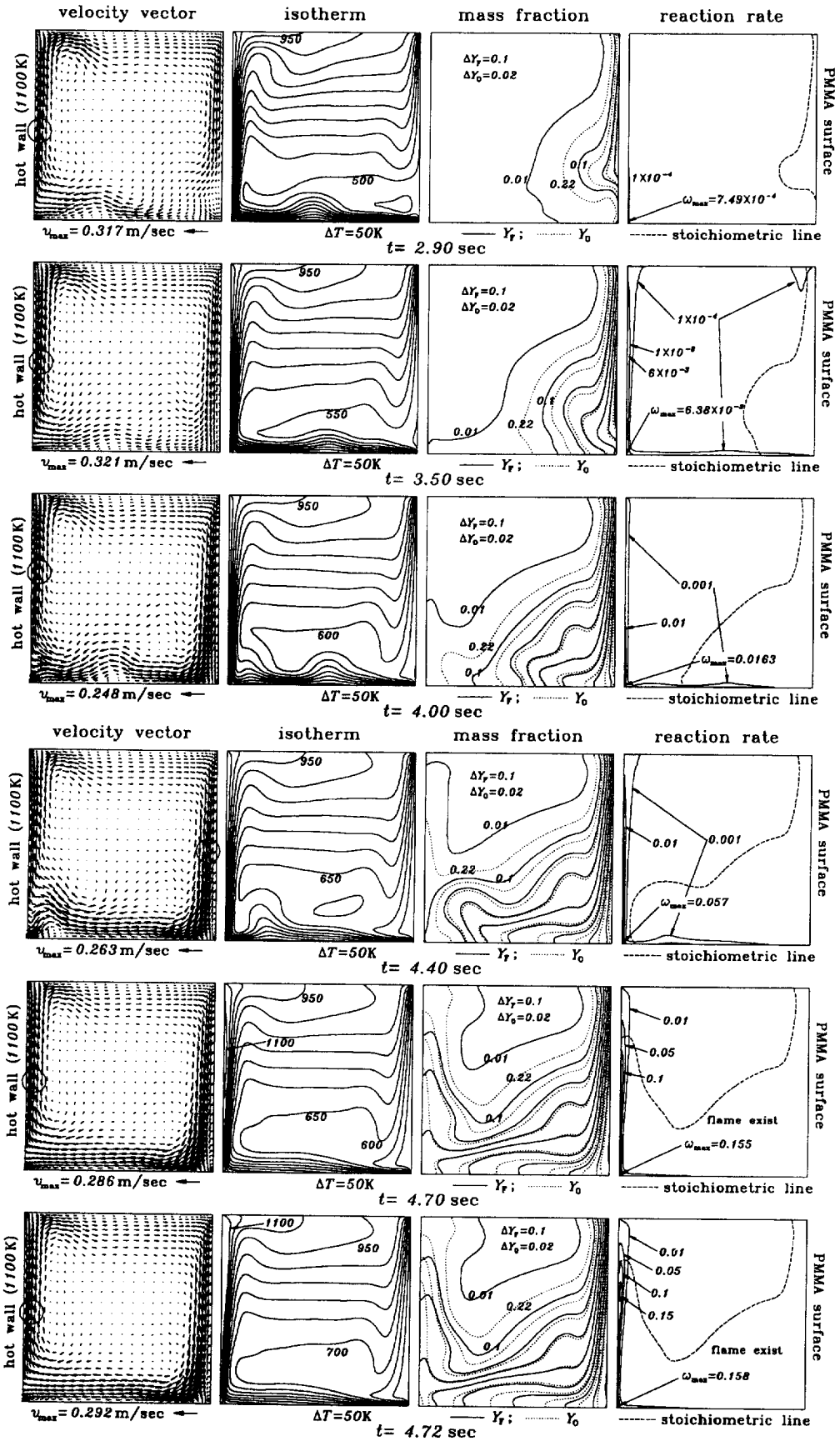

Fig. 3. Temporal variations of velocity vector, isotherm, fuel and oxidizer mass fractions and reaction rate with stoichiometric line for hot wall temperature, T_h = 1100 K.

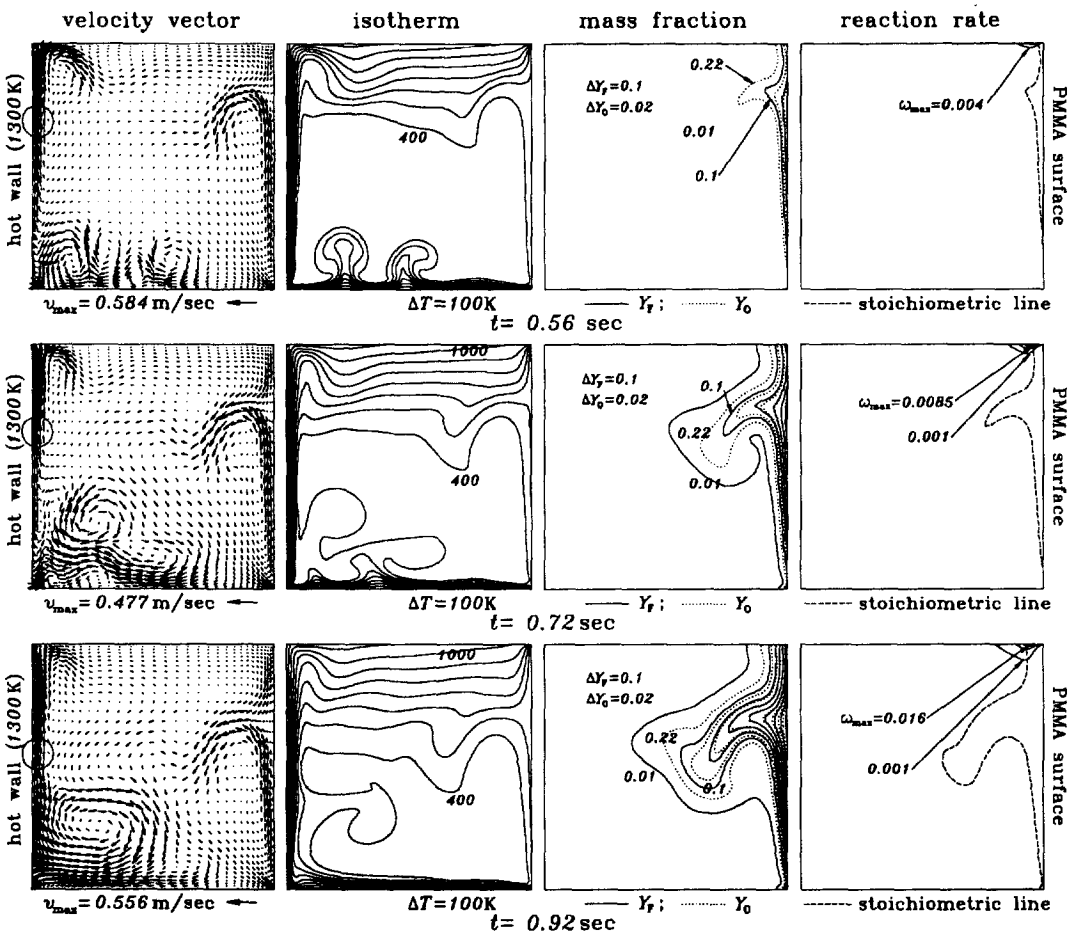

Fig. 4. Temporal variations of velocity vector, isotherm, fuel and oxidizer mass fractions and reaction rate with stoichiometric line for hot wall temperature, T_h = 1300 K.

as shown in the figure. Afterwards, as the hot gas originating from the hot wall is supplied into the region near the PMMA wall, the sign of Nu^C is reversed. As the PMMA is heated, it begins to be pyrolysed, thus increasing the absolute value of Nu^P.

The rate of devolatilization is well shown in the figure of v_P. When the mean temperature T_P reaches 470 K, the ejecting velocity of the volatile gas corresponds to about 0.001 m s^{-1} and thereafter it increases.

Figure 6 illustrates a summary of the ignition mechanism considered to take place in this geometry for various hot wall temperatures, T_h. For values of T_h lower than 900 K, no ignition is observed. For cases in which 900 K < T_h < 1100 K, the thermally decomposed volatile gas migrates toward the hot wall region, while mixing with the oxidizer. The ignition is thus mainly controlled by a mixing process of volatile gas with air, and ignition occurs near the hot wall region. However, for cases in which T_h > 1100 K, the hot air originating from the hot wall region migrates to the PMMA wall region where the volatile gas is about to diffuse out. Consequently, ignition occurs in the PMMA region. This ignition is considered to be thermally controlled.

4. CONCLUSIONS

Ignition phenomenon of a devolatilizing solid fuel in a confined geometry is considered to be a very important topic in the area of fire safety. However, due to its inherent formidability in the various physical processes involved, it has not yet been fully addressed. In this work, a numerical study has been performed to analyse the radiative and free convective ignition of a PMMA wall in a confined rectangular enclosure. The ignition mechanism has been discussed for various hot wall temperatures, T_h, with surface radiation included.

The unstable nature of fluid motion due to buoyancy has been observed at the floor region, which is initially heated by surface radiation from the hot wall. Eventually it induced a very complicated recirculating flow pattern inside the enclosure, which then affects the mixing of fuel and oxidizer. No ignition takes place when the hot wall temperature is lower than 900 K. For the case of 950 K < T_h < 1100 K, the thermally decomposed volatile gas at the PMMA wall migrates into the hot wall region, assisted by convective fluid flow. After being mixed with oxidizer, it ignites there in the hot wall region. This ignition pro-

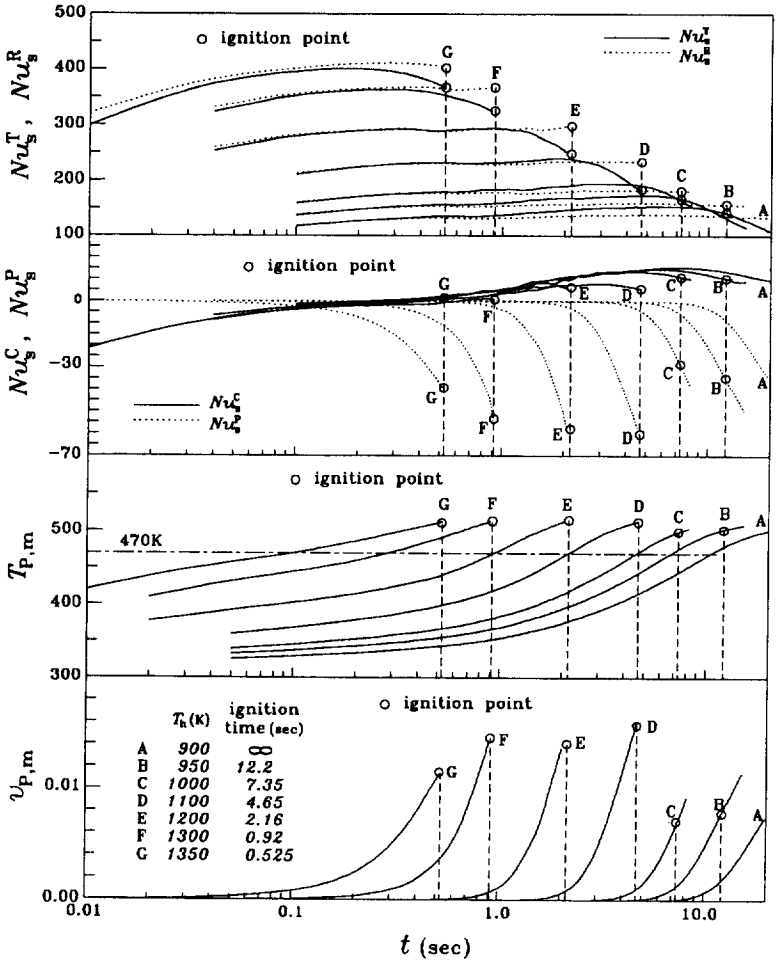

Fig. 5. Temporal variations of Nusselt number, mean temperature and mean ejecting velocity of volatile gas at the PMMA surface.

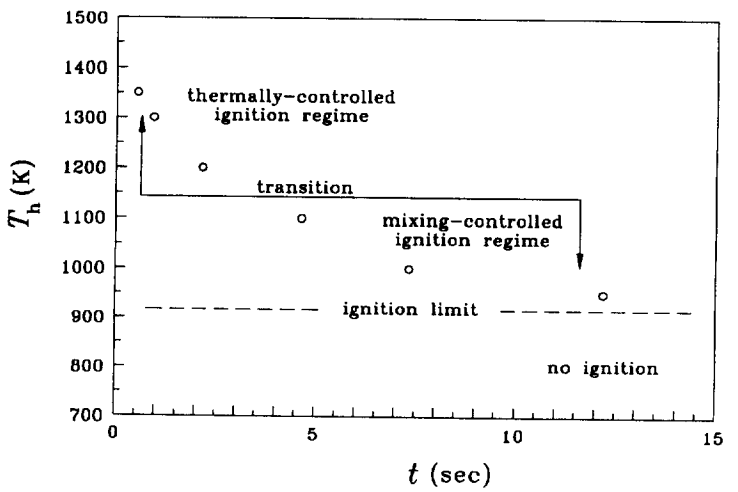

Fig. 6. Schematic illustration of ignition mechanism for various hot wall temperatures.

cess is considered to be controlled by the mixing and transport of fuel and oxidizer. However, for $T_h > 1100$ K, ignition was controlled by the infiltration of hot gas originating from the hot wall into the fuel vapor region created near the PMMA wall.

From the calculation results, the internal flow pattern and ignition mechanism depend strongly on the specific configuration thus further geometries such as containing obstacles and round corners remain to be studied.

Acknowledgements—This paper was supported (in part) by Non Directed Research Fund, Korea Research Foundation.

REFERENCES

1. D. L. Simms, Experiments on the ignition of cellulosic materials thermal radiation, *Combust. Flame* **5,** 369–375 (1961).
2. S. Martin, Diffusion-controlled ignition of cellusoic materials by intense radiant energy, *Proceedings of the 10th International Symposium on Combustion*, pp. 877–896. The Combustion Institute, Pittsburgh (1965).
3. N. J. Alvares, P. L. Blackshear, Jr and A. M. Kanury, The influence of free convection on the ignition of vertical cellulosic panels by thermal radiation, *Combust. Sci. Technol.* **1,** 407–413 (1970).
4. T. Kashiwagi, A radiative ignition model of a solid fuel, *Combust. Sci. Technol.* **8,** 225–236 (1974).
5. T. Kashiwagi, Effect of sample orientation on radiative ignition, *Combust. Flame* **44,** 223–245 (1981).
6. P. D. Gandhi and A. M. Kanury, Criterion for spontaneous ignition of radiantly heated organic solids, *Combust. Sci. Technol.* **50,** 233–254 (1986).
7. S. H. Park and C. L. Tien, Radiation induced ignition of solid fuels, *Int. J. Heat Mass Transfer* **33,** 1511–1520 (1990).
8. S. W. Baek and J. S. Kim, Ignition of a pyrolysing solid with radiatively active fuel vapor, *Combust. Sci. Technol.* **75,** 89–102 (1991).
9. G. N. Ivey, Experiments on transient natural convection in a cavity, *J. Fluid Mech.* **144,** 389–401 (1984).
10. C. Vovelle, J. L. Delfau, M. Reuillon, J. Bransier and N. Laraqui, Experimental and numerical study of the thermal degradation of PMMA, *Combust. Sci. Technol.* **53,** 187–201 (1987).
11. B. Amos and A. C. Fernandez-Pello, Model of the ignition and flame development point flow: ignition by vapor fuel radiation absorption, *Combust. Sci. Technol.* **62,** 331–343 (1989).
12. K. C. Karki and S. V. Pakankar, Pressure based calculation procedure for viscous flows at all speeds in arbitrary configurations, *AIAA J.* **27,** 1167–1174 (1989).
13. T. Hayase, J. A. C. Humphrey and R. Greif, Consistently formulated QUICK scheme for fast and stable convergence using finite volume iterative calculation procedures, *J. Comput. Phys.* **98,** 108–118 (1992).
14. T. Y. Kim, Analysis on the radiative and convective ignition of the solid fuel in a confined rectangular enclosure, Ph.D. Thesis, Department of Aerospace Engineering, Korea Advanced Institute of Science and Technology, Taejon, Korea (1993).